





Phage-Resistant Bacteria Reveal a Role for Potassium in Root Colonization

 Elhanan Tzipilevich,^{a,b}  Philip N. Benfey^{a,b}

^aHoward Hughes Medical Institute, Duke University, Durham, North Carolina, USA

^bDepartment of Biology, Duke University, Durham, North Carolina, USA

ABSTRACT Bacteriophage predation is an important factor in bacterial community dynamics and evolution. Phage-bacterium interaction has mainly been studied in lab cultures, while dynamics in natural habitats, and especially in the plant root niche, are underexplored. To better understand this process, we characterized infection of the soil bacterium *Bacillus subtilis* NCBI 3610 by the lytic phage SPO1 during growth in LB medium and compared it to root colonization. Resistance *in vitro* was primarily through modification of the phage receptor. However, this type of resistance reduced the ability to colonize the root. From a line that survived phage infection while retaining the ability to colonize the root, we identified a new phage resistance mechanism involving potassium (K⁺) ion influx modulation and enhanced biofilm formation. Furthermore, we show that potassium serves as a stimulator of root colonization among diverse growth-promoting bacilli species, with implications for plant health.

IMPORTANCE Bacteriophage predation is an important factor in bacterial community dynamics and evolution. Phage-bacterium interaction has mainly been studied in lab cultures, while dynamics in natural habitats, and especially in the plant root niche, are underexplored. To better understand this process, we characterized infection of the soil bacterium *Bacillus subtilis* NCBI 3610 by the lytic phage SPO1 during growth in LB medium and compared it to root colonization. Resistance *in vitro* was primarily through modification of the phage receptor. However, this type of resistance reduced the ability to colonize the root. From a line that survived phage infection while retaining the ability to colonize the root, we identified a new phage resistance mechanism involving potassium (K⁺) ion influx modulation and enhanced biofilm formation. Furthermore, we show that potassium serves as a stimulator of root colonization among diverse growth-promoting bacilli species, with implications for plant health.

KEYWORDS *Bacillus subtilis*, bacteriophage, evolution, biofilms, plant-microbe interactions

Plant roots are associated with diverse bacteria in the soil (1), which can affect many aspects of plant life, including root architecture (2), nutrient acquisition (3), and disease state (2, 4). The root rhizosphere, i.e., the area close to the root surface, is enriched with specific bacterial taxa in comparison to that in bulk soil. This unique microbial composition is determined by the soil surrounding the plant root and its preexisting bacterial diversity (5, 6) and plant genotype (7) as well as the interaction with other bacteria (8) and with phage (9). Although a large body of research has been conducted to characterize each of these factors, the whole picture, and especially the role of phage in bacterial root colonization, is far from complete.

Phage are viruses that infect and kill bacteria (10, 11). As bacterial predators, they influence bacterial community dynamics through elimination of their sensitive hosts. Bacteria, in turn, respond by rapid evolution of phage resistance (12). In addition to influencing bacterial interaction with phage, newly acquired resistance (10, 13) can

Citation Tzipilevich E, Benfey PN. 2021. Phage-resistant bacteria reveal a role for potassium in root colonization. *mBio* 12:e01403-21. <https://doi.org/10.1128/mBio.01403-21>.

Editor Gustavo H. Goldman, Universidade de Sao Paulo

Copyright © 2021 Tzipilevich and Benfey. This is an open-access article distributed under the terms of the [Creative Commons Attribution 4.0 International license](https://creativecommons.org/licenses/by/4.0/).

Address correspondence to Philip N. Benfey, philip.benfey@duke.edu.

Received 12 May 2021

Accepted 13 July 2021

Published 17 August 2021

also cause changes in colony morphology (14), genome-wide mutation rate (15), and lateral spread of genetic material (16). In recent years, insights have been gained into how phage-bacterium interactions affect bacterial growth in ocean (17) and mammalian gut ecosystems (18). However, little is known about the effects of phage-bacterium interactions in other ecosystems, especially in soil and the root rhizosphere (19).

To address this question, we utilized *Bacillus subtilis* strain NCBI 3610 (henceforth, *B. subtilis*) (20) and its cognate lytic phage SPO1 (21) to explore their interaction during root colonization of the plant model system *Arabidopsis thaliana*. *B. subtilis* is a Gram-positive spore-forming bacterium isolated from soil and is able to colonize plant roots (22). Root colonization by *B. subtilis* is mediated by formation of a biofilm on the root (23). Biofilms are bacterial communities encased in an extracellular matrix. The *B. subtilis* matrix is mainly composed of sugar polymers, encoded by the *eps* operon, and protein fibers encoded by the *tapA-sipW-tasA* operon (24). *B. subtilis* defective in biofilm formation exhibits severe defects in root colonization (23). The phage SPO1 is a lytic phage, representing a large and diverse group of *Myoviridae* bacteriophages, harboring a long contractile tail. SPO1 phage exhibits a complex infection cycle, involving the subversion of the host transcription machinery for its own use (25). SPO1 utilizes the wall teichoic acid polymers (WTAs) as receptors to invade *B. subtilis* cells (26). WTAs are long sugar polymers that are incorporated into the cell wall and membrane of *B. subtilis* and other Gram-positive bacteria (27). SPO1 binds these polymers when they are decorated by glucose moieties (gWTAs). Comparison of phage-bacterium evolution upon infection in LB medium and during root colonization revealed that phage infection *in vitro* and *in planta* exhibits different evolutionary trajectories. Characterization of bacteria resistant to phage infection during root colonization led to the identification of a novel phage resistance mechanism through modulation of potassium (K^+) ion influx and enhanced biofilm formation. Furthermore, we show that potassium serves as a stimulator of root colonization among diverse bacilli species.

RESULTS

Loss of phage receptor results in a fitness cost for root colonization. To explore phage-bacterium interactions during root colonization, we inoculated the roots of *A. thaliana* with *B. subtilis* 3610 bacteria together with SPO1 phage at either a high (phage/bacteria, 1:1), or low (phage/bacteria, 1:10) multiplicity of infection (MOI). Measuring bacterial colonization (CFU) after 48 h revealed a reduction in root colonization of ~95% at an MOI of 1 and an ~90% reduction at an MOI of 0.1 (Fig. 1A), indicating that SPO1 can efficiently infect and kill its host bacteria during root colonization. Significant levels of PFU were recovered from the root after SPO1 infection ($5.56 \times 10^4 \pm 4.67 \times 10^4$, for MOI of 1, $n=6$). However, no increase in the amount of the phage was observed in comparison to the input (PFU = 10^6), probably reflecting the fact that phage cannot adhere to the root without the presence of the host bacteria. Selection pressure by phage drives bacterial evolution of resistance mechanisms (28). To explore the evolution of phage resistance mechanisms *in vitro* versus those *in planta*, we isolated 300 bacteria (screen 1) that survived phage infection on the root and restreaked them on agar plates containing SPO1 phage, (maximum of 10 bacteria from each root). We found 20 *in planta* survivors that became resistant to phage infection *in vitro*. On the other hand, 100% of 70 bacteria isolated after surviving phage infection in LB medium (taken from 3 independent LB plates) became immune to further infection. Twenty randomly selected *in vitro* survivors became phage resistant through loss of the phage receptor, as judged by a lack of staining with concanavalin A, Alexa Fluor 488 conjugate (ConA₄₈₈), a lectin that binds specifically glycosylated WTA (gWTA) (Fig. 1B) (see also reference 26). Of the 20 SPO1-resistant bacteria isolated from the plant all but one (m28) had lost their ability to recolonize the root (Fig. 1C). Nineteen of these isolates concomitantly lost their ConA₄₈₈ staining (see Fig. S1A in the supplemental material). One of the isolates, m28, was completely phage resistant *in vitro* when infected in liquid culture (Fig. S1B) but still exhibited faint ConA₄₈₈ staining (Fig. S1A and C) and partial sensitivity when infected on roots (Fig. 2A). The correlation between SPO1 sensitivity and root colonization ability suggests that gWTA is important

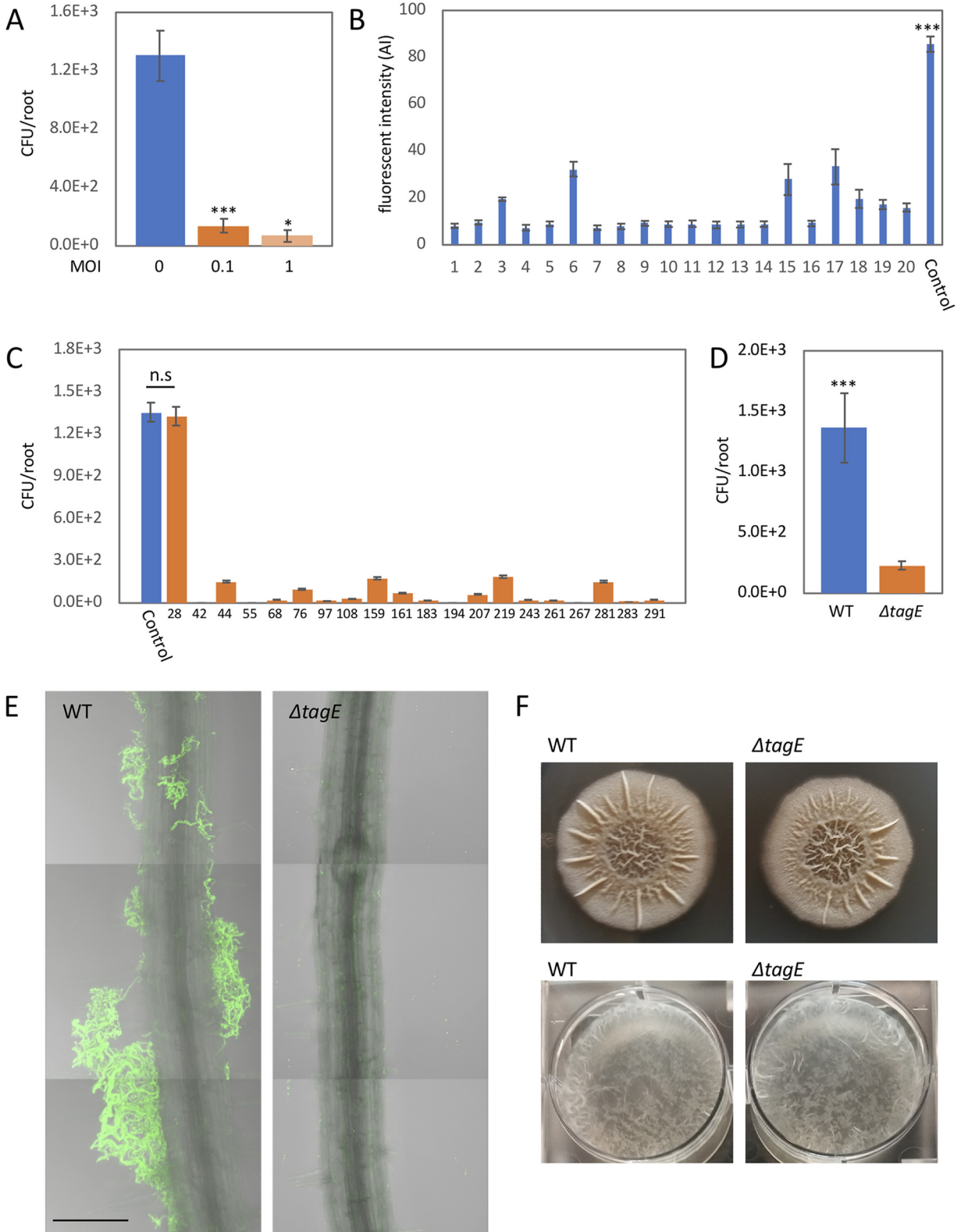


FIG 1 SPO1 phage receptor is necessary for bacterial root adhesion. (A) Seedlings were inoculated with *B. subtilis* 3610 together with SPO1 phage, at either a high (phage/bacteria, 1:1) or low (phage/bacteria, 1:10) multiplicity of infection (MOI) or with no phage (MOI of 0) for 48 h on agar plates, and the number of colonizing bacteria was counted. Shown are averages and standard deviations (SDs) from 2 independent experiments with an *n* of ≥3 for each (*n* throughout the paper is the number of roots sampled [biological replicates] with 3 technical replicates from each root). *, *P* < 0.05; ***, *P* < 0.005. (B) Twenty randomly selected bacterial colonies that survived SPO1 infection were stained with ConA₄₈₈ and observed under a compound microscope. Shown are average and SD fluorescent intensity values of 10 bacteria (Continued on next page)

for efficient root colonization. To test this hypothesis, we inoculated roots with $\Delta tagE$ bacteria, which lack gWTA (29), and found a significant reduction in root colonization by CFU measurement and fluorescent bacteria (Fig. 1D and E). Because biofilm formation has been shown to be necessary for root colonization by *B. subtilis* (30), we tested the ability of $\Delta tagE$ bacteria to form a biofilm *in vitro*. $\Delta tagE$ cells exhibit normal biofilm formation both on agar plates and in liquid medium (Fig. 1F). Of note, gWTA is required for nasal epithelium colonization by *Staphylococcus aureus* (31). Our results suggest that gWTA in *B. subtilis* is similarly important for plant surface adhesion, irrespective of biofilm formation.

Bacteria evolved a novel phage resistance mechanism. Our results indicate that loss of the phage receptor results in a fitness cost to bacteria during root colonization. To identify alternative pathways utilized by bacteria to resist phage infection during root colonization, we utilized the bacteria that survived phage infection on the root (100 of the 300 bacteria from screen 1) and infected them with SPO1, this time during root colonization (screen 2). Most of the bacteria exhibited phage sensitivity similar to that of the parental bacteria. However, of 100 bacterial strains tested, we found 4 that survived SPO1 infection on roots better than wild-type (WT) cells (Fig. 2A). To explore the mechanism of bacterial survival, we sequenced the genomes of m5, m11, m54, and m93, the 4 bacteria isolated during screen 2, along with m28 isolated from screen 1. Table 1 presents the mutations in each of the bacteria.

m28 and m93 harbor mutations in *gtaB* and *tagE*, genes involved in the WTA glycosylation pathway (27). Interestingly, m11 and m54 do not have mutations in genes previously implicated in WTA glycosylation but nonetheless exhibited complete (m54) and partial (m11) loss of ConA₄₈₈ staining (Fig. 2B and Fig. S1C). m11, m54, and m93 exhibited phage resistance *in vitro* (Fig. S1B).

One mutant, m5, exhibited enhanced phage resistance when infected *in planta* at a medium MOI (1 to 0.1) (Fig. 2C, CFU, and Fig. 2D, fluorescent bacteria), phage sensitivity *in vitro*, and ConA₄₈₈ staining similar to that of WT (Fig. 2B and E and Fig. S2B), indicating that it harbors a novel phage resistance mechanism. The m5 mutant also exhibited enhanced resistance to infection by SPP1, a lytic phage from a different bacteriophage family (*Siphoviridae*) (Fig. 2F). SPP1 utilizes YueB, a membrane protein, as a receptor. However, gWTA also plays an important role for SPP1 infection as well (32). Nevertheless, m5 has a resistance mechanism that is not phage-family specific. m5 harbors a single point mutation in the *ktrC* gene, encoding a low-affinity potassium channel. This missense mutation changes proline 189 into threonine (KtrC P189T) and resides in a conserved RCK domain, known to bind the regulatory molecule ci-di-AMP (33, 34). ci-di-AMP negatively regulates potassium uptake (35). We hypothesized that KtrC P189T is a gain of function mutation, affecting the regulation of potassium uptake.

Potassium enhances root colonization and phage resistance through modulation of biofilm formation. Several potassium channels are encoded in the *B. subtilis* genome: *ktrAB* and *kimA* encode high-affinity channels (36, 37), while the *ktrCD* operon encodes a low-affinity channel (36). To understand the effect of the KtrC P189T mutation and potassium uptake on bacterial root colonization, we examined the colonization efficiency of bacteria lacking these channels. While $\Delta ktrC$ and $\Delta kimA$ mutants colonized the root with similar efficiency to WT bacteria (Fig. 3A), $\Delta ktrA$ bacteria exhibited reduced root colonization (Fig. 3A). The KtrC P189T mutation is able to restore the colonization of $\Delta ktrA$ bacteria (Fig. 3A, M5 $\Delta ktrA$), suggesting that this mutation enhances potassium uptake through the KtrC channel. Growing plants on media with different levels of potassium revealed a positive correlation between potassium concentration and root colonization

FIG 1 Legend (Continued)

from each of the colonies. ***, $P < 0.005$. (C) Twenty isolated SPO1 resistant bacteria were inoculated on seedlings and grown for 48 h, and the number of colonizing bacteria were counted. Shown are averages and SDs with an n of ≥ 3 . (D) Seedlings were inoculated with either WT or $\Delta tagE$ bacteria for 48 h, and the number of colonizing bacteria was counted. Shown are averages and SDs from 2 independent experiments with an n of ≥ 3 for each. ***, $P < 0.005$. (E) Seedlings were inoculated with either WT or $\Delta tagE$ bacteria expressing green fluorescent protein (GFP) (*amyE::P_{immE}-gfp*) for 48 h on agar plates. Shown are representative overlay $\times 200$ magnification confocal images of differential interference contrast (DIC) (root) and GFP fluorescence (bacteria). Scale bar, 50 μm . (F) WT and $\Delta tagE$ bacteria were inoculated onto MSgg agar plates (top) or liquid medium (bottom). Shown are representative biofilm images.

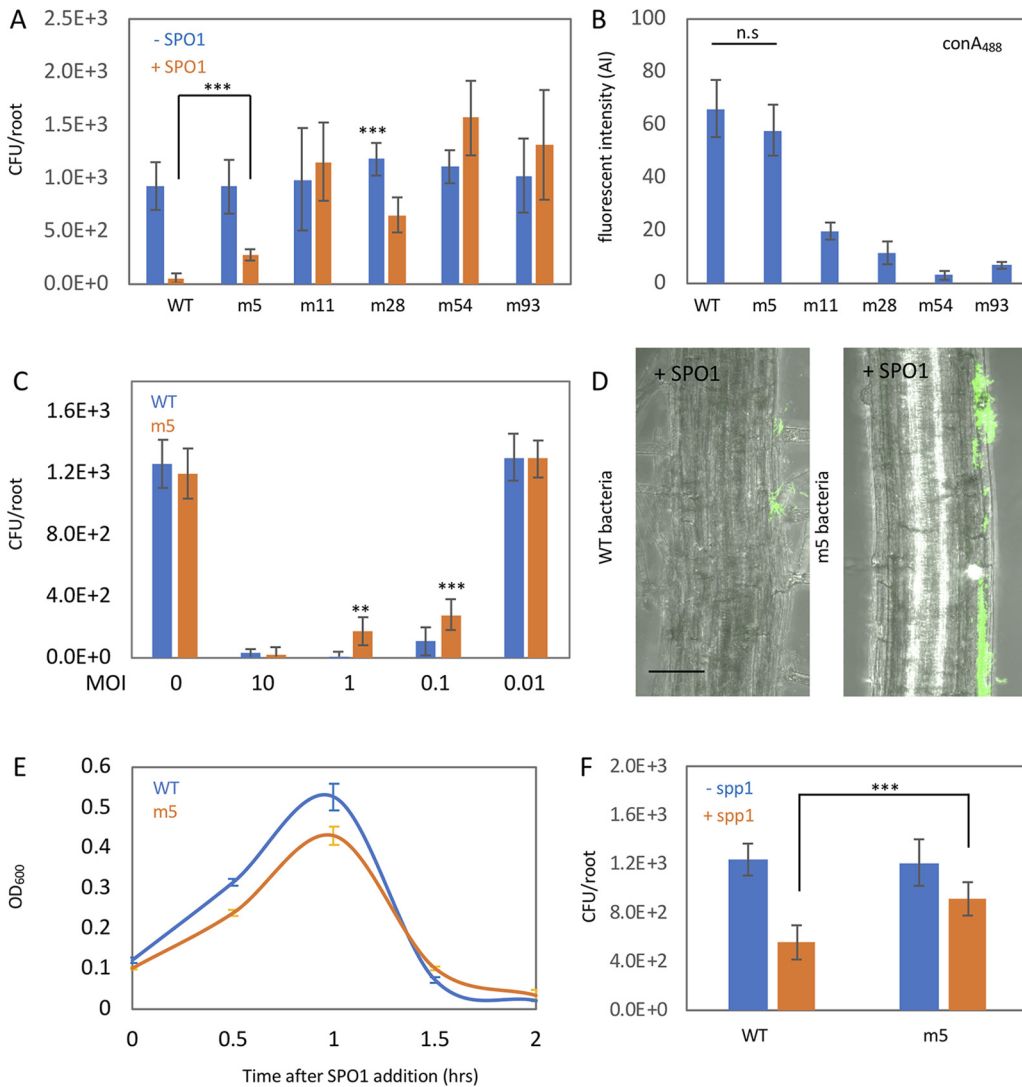


FIG 2 A novel SPO1 resistance mechanism. (A) Seedlings were inoculated with the indicated bacterial strains, with or without SPO1 addition, for 48h on agar plates, and the number of colonizing bacteria was counted. Shown are averages and SDs from 2 independent experiments with an n of ≥ 3 for each. ***, $P < 0.005$. (B) Bacterial strains were stained with ConA₄₈₈ and observed under the microscope. Shown are average and SD of fluorescence intensity values of 10 bacteria from each colony. n.s., not significant. (C) Seedlings were inoculated with either WT or m5 bacteria, with the indicated phage MOI, for 48h on agar plates, and the number of colonizing bacteria was counted. Shown are averages and SDs from 2 independent experiments with an n of ≥ 3 for each. **, $P < 0.01$; ***, $P < 0.005$. (D) Seedlings were inoculated with either WT or m5 bacteria expressing GFP (*amyE::P_{mmE}-gfp*), in the presence of SPO1, for 48h on agar plates. Shown are representative overlay $\times 200$ magnification confocal images of DIC (root) and GFP fluorescence (bacteria). Scale bar, 20 μ m. (E) WT and m5 bacteria were infected with SPO1 in LB medium, and OD₆₀₀ was followed. Shown are averages and SDs, $n = 3$. (F) Seedlings were inoculated with either WT or m5 bacteria, with or without SPP1 phages, for 48h on agar plates, and the number of colonizing bacteria was counted. Shown are averages and SDs from 2 independent experiments with an n of ≥ 3 for each. ***, $P < 0.005$.

by WT bacteria (Fig. 3B), with the effect plateauing at 10 mM. Similarly, root colonization on 0.25 Murashige and Skoog (MS) plates, with addition of 5 mM potassium (KCl) (equal to total of ~ 10 mM) indicated a positive effect of potassium on root colonization (Fig. 3C). Stimulation of root colonization was specific to potassium ions, as neither sodium nor nitrogen had a similar effect (Fig. S2A). Simply adding extra potassium to the plant growth medium was sufficient to enhance survival of WT cells upon phage infection (Fig. 3C and D), reinforcing the idea that the *KtrC* P189T mutation affects phage infection through increased potassium uptake.

It was previously shown that *B. subtilis* bacteria sense potassium influx through the cell membrane, utilizing KinC and KinB protein kinases to induce biofilm formation

TABLE 1 Bacterial strains

| Bacterial strain | Mutation |
|------------------|--|
| m5 | Missense mutation in KtrC P189T |
| m11 | Mutations in YwbO promoter |
| m28 | Missense mutation GtaB Y170S |
| m54 | Missense mutations in YwrK T334S and CdaA F97L |
| m93 | Frame shift in <i>tagE</i> T1013 leading to premature stop codon |

genes and sliding motility, respectively (38, 39). Both biofilm formation and sliding motility play important roles during root colonization (23, 40). We found that m5 $\Delta kinC$ bacteria, but not m5 $\Delta kinB$ bacteria, lost SPO1 resistance (Fig. 3E). Addition of potassium to the plant growth medium failed to stimulate phage resistance for $\Delta kinC$ bacteria (Fig. S2C). Thus, we conclude that KinC is involved in the effect of potassium on root colonization and phage resistance.

KinC activation induces a phosphorylation cascade that culminates in induction of biofilm matrix genes (38). Disruption of the biofilm matrix operons *epsA-O* and *tapA-sipW-tasA* abolished the effect of potassium on root colonization (Fig. S2C). Interestingly, disruption of the *tapA-sipW-tasA* operon, but not *epsA-O*, reduced the phage resistance phenotype of m5 cells (Fig. 3F and G), suggesting that an increase in the protein fiber component was responsible for the phage resistance effect of increased potassium influx. Thus, our analysis revealed a novel phage adaptation mechanism that works through enhanced potassium influx by stimulating biofilm matrix formation.

To further characterize the role of biofilm matrix formation in phage resistance, we monitored SPO1 infection during biofilm formation *in vitro* (20). Measurement of biofilm diameter on MSgg agar plates revealed significant reduction in colony diameter on plates containing SPO1 phage (Fig. 4A). Of note, $\Delta ktrA$ cells, although able to form normal biofilm in the absence of phage, exhibited a significant decrease in biofilm diameter in the presence of phage in comparison to that of WT infected cells (Fig. 4A and B). Similar to what was observed in plants, the KtrC P189T mutation was able to compensate for the increased sensitivity of $\Delta ktrA$ cells (Fig. 4A and B). Thus, our *in vitro* analysis provides further support for the hypothesis that potassium influx modulates biofilm formation to enhance phage resistance. Equivalent results were obtained for pellicle biofilm formation on liquid MSgg medium (Fig. S3), where enhanced potassium influx in m5 bacteria, or addition of extra potassium to the medium of WT bacteria, increased the chance of surviving SPO1 infection, while decreased influx, due to the $\Delta ktrA$ mutation, increased phage sensitivity.

Potassium enhances root colonization by diverse bacilli species. To determine if potassium is able to enhance colonization by other bacilli species, we analyzed its effect on *Bacillus velezensis* FZB42, a plant-associated bacterium (41), shown to enhance plant health through growth stimulation and pathogen inhibition. We found that potassium enhances root colonization of *B. velezensis* FZB42 (Fig. 5A), and this phenomenon was abolished in *B. velezensis* FZB42 $\Delta kinC$ cells (Fig. 5B). A similar phenomenon was observed for *B. subtilis* GB03 and *B. pumilus* SE34, two other plant growth-promoting bacteria (Fig. 5A). Thus, potassium serves as a wide-spread signal, stimulating root colonization by diverse bacilli species. *B. velezensis* FZB42 inhibits the growth of the plant fungal pathogen *Rhizoctonia solani* (42), raising the possibility that simply adding potassium to the growth medium could enhance *B. velezensis* FZB42 colonization and fungal protection. Indeed, potassium enhanced plant growth when inoculated with *Rhizoctonia solani* in the presence of *B. velezensis* FZB42 in comparison to growth of plants inoculated with fungi but no bacteria (Fig. 5C), and this effect of plant protection was abolished in $\Delta kinC$ cells, which are unable to sense potassium influx (Fig. 5C).

DISCUSSION

Phage infection has been extensively characterized in lab cultures. Recent work revealed that phage-bacterium interactions in natural environments can differ significantly from those

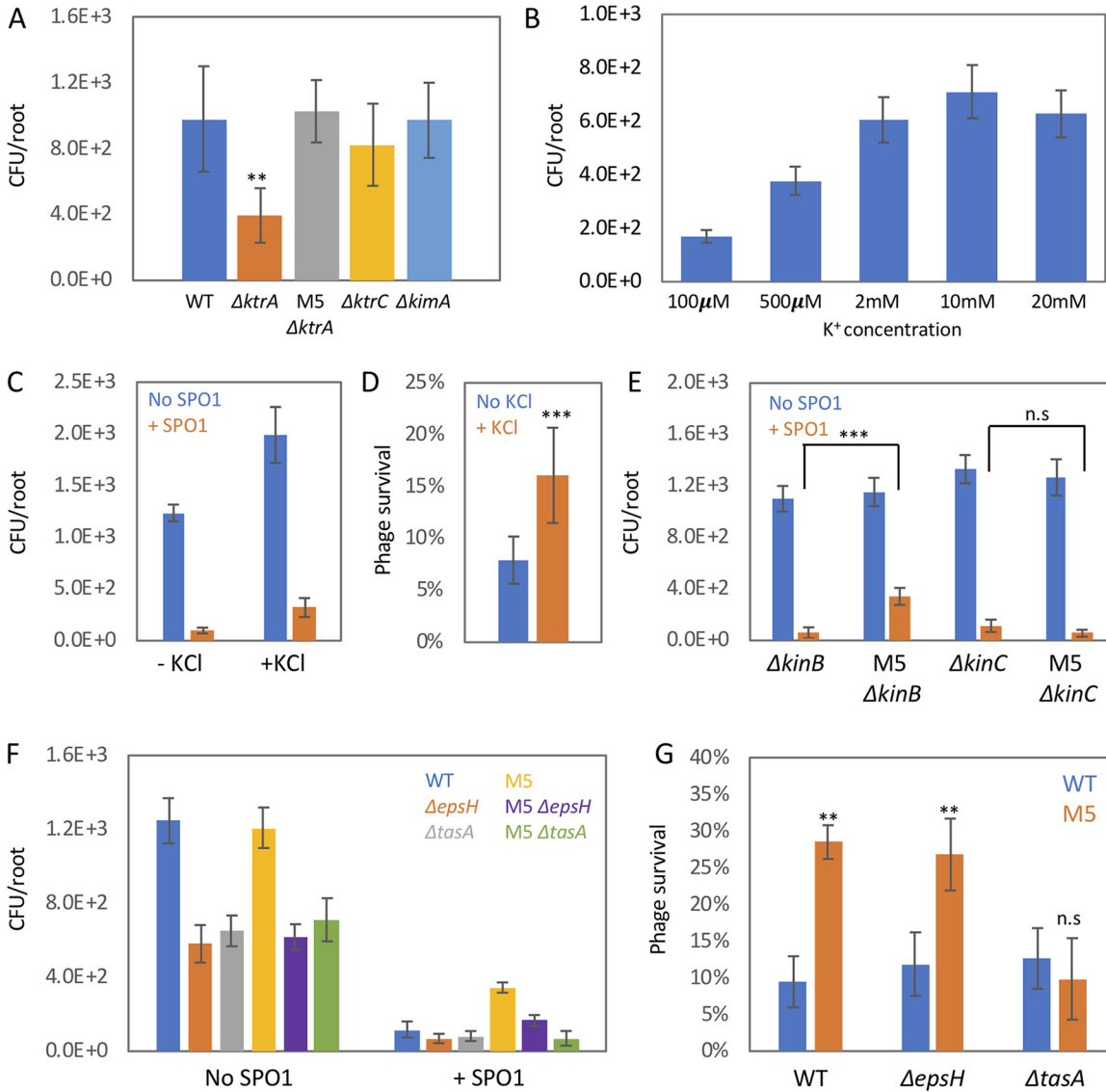


FIG 3 Potassium modulates *B. subtilis* root colonization and phage resistance through biofilm formation. (A) Seedlings were inoculated with the indicated bacterial strains for 48 h on agar plates, and the number of colonizing bacteria was counted. Shown are averages and SDs from 2 independent experiments with an *n* of ≥ 3 for each. **, *P* < 0.01. (B) Seedlings were inoculated with WT *B. subtilis* on MS agar plates supplemented with the indicated potassium concentration for 48 h, and the number of colonizing bacteria was counted. Shown are averages and SDs from 2 independent experiments with an *n* of ≥ 3 for each. (C and D) Seedlings were inoculated with WT *B. subtilis*, with or without SPO1 addition, for 48 h on 0.25 \times MS agar plates in the presence or absence of 5 mM KCl, and the number of colonizing bacteria was counted. Shown are averages and SDs of CFU values (C) and the percentages of SPO1 survival (D), from 2 independent experiments with an *n* of ≥ 3 for each. ***, *P* < 0.005. (E) Seedlings were inoculated with the indicated bacterial strains, with or without SPO1 addition, for 48 h on agar plates, and the number of colonizing bacteria was counted. Shown are averages and SDs from 2 independent experiments with an *n* of ≥ 3 for each. ***, *P* < 0.005. (F and G) Seedlings were inoculated with the indicated bacterial strains, with or without SPO1 addition, for 48 h on agar plates in the presence or absence of 5 mM KCl, and the number of colonizing bacteria was counted. Shown are average and SD CFU values (F) and percentages of SPO1 survival (G) from 2 independent experiments with an *n* of ≥ 3 for each, **, *P* < 0.01.

observed in the lab (43) due to the fitness constraints encountered by bacteria in their natural environment. This can impede the evolution of phage receptors, the main resistance pathway observed in the lab (44). We found that gWTA, the SPO1 phage receptor, is essential for root adhesion; thus, receptor modification has a fitness cost in the root environment. Of note, it has been shown that gWTA is essential for adhesion of *Staphylococcus aureus* to the nasal epithelium (31), while gWTA also serves as phage receptor for several *S. aureus*-infecting phages (45). It will be interesting to determine if phage-bacterium evolution is constrained in this niche as well.

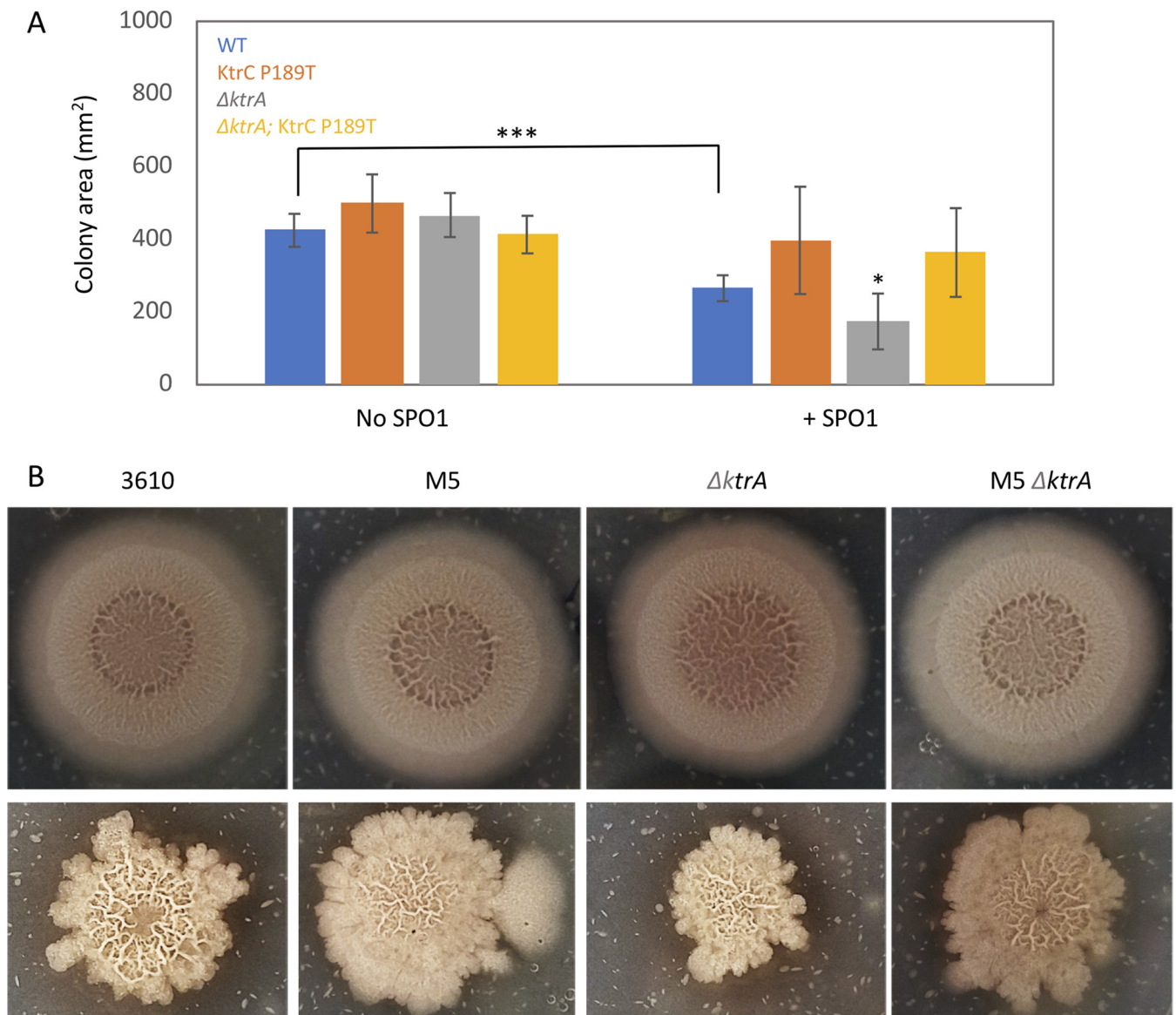


FIG 4 Potassium modulates phage resistance during biofilm formation *in vitro*. (A) The indicated bacterial strains were inoculated onto MSgg agar plates with or without SPO1 addition for 48 h, and colony area was measured. Shown are averages and SDs from an n of 6. *, $P < 0.05$; ***, $P < 0.005$. (B) Shown are representative images for the experiment described for panel A with (bottom) or without (top) SPO1 addition.

While evolution of receptor modification is not favored, we found that bacteria in the root adapt to phage infection through evolution of enhanced biofilm formation. Consistent with previous *in vitro* work (38), we show that during plant colonization, altering potassium efflux through KtrCD channels enhances *B. subtilis* biofilm formation and thus promotes survival upon phage infection (Fig. 6). Our results indicate that protein fiber density, encoded by the *tapA-sipW-tasA* operon, is the main determinant of SPO1 resistance. Interestingly, it has been shown that curli protein fibers are important for T7 resistance in a biofilm of *Escherichia coli* bacteria (46). Phage-bacterium interaction in biofilm is an emerging area of research (47). Biofilms are an important mode of life for bacteria colonizing natural environments, such as plant roots, as well as for pathogenic bacteria (48). Thus, in order to understand bacterial community dynamics in nature, and to deal with biofilm pathogenicity, it is important to explore the interaction of phage and bacteria in this specific niche.

Phage utilize bacterial appendages decorating the cell surface as receptors. Appendages such as flagella, type IV pili, exopolysaccharides, and transporters of nutrients, are important

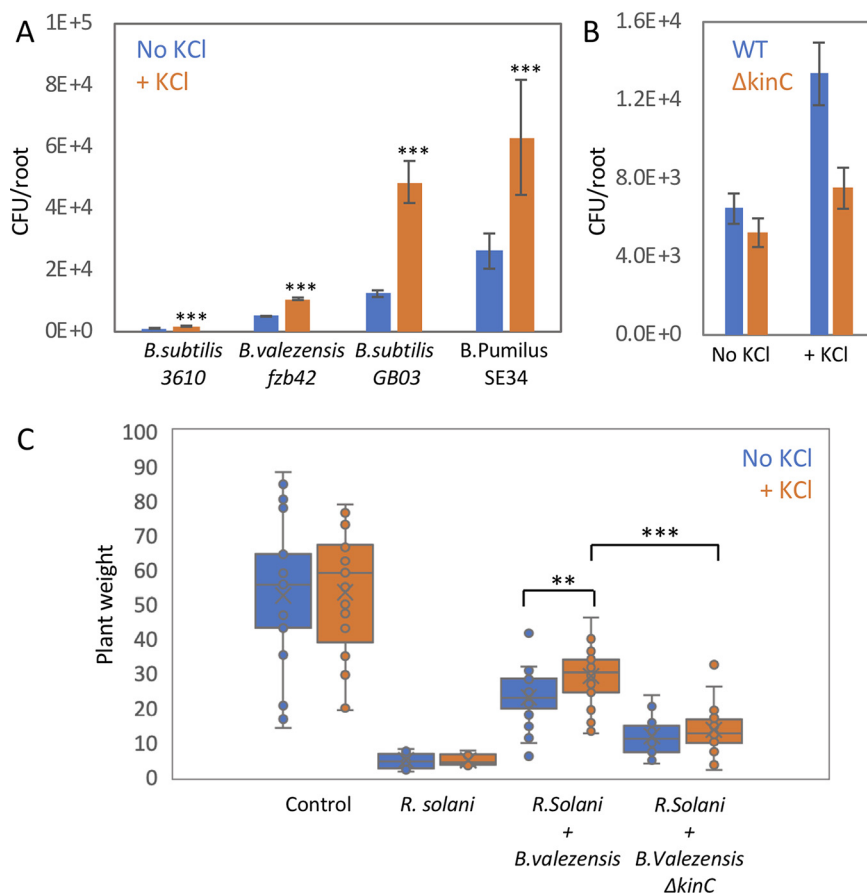


FIG 5 Potassium modulates root colonization by diverse bacillus species. (A) Seedlings were inoculated with the indicated bacterial species for 48 h on 0.25× MS agar plates in the presence or absence of 5 mM KCl, and the number of colonizing bacteria was counted. Shown are averages and SDs from 2 independent experiments with an n of ≥ 3 for each. ***, $P < 0.005$. (B) Seedlings were inoculated with either WT or $\Delta kinC$ *B. velezensis* FZB42 bacteria for 48 h on 0.25× MS agar plates in the presence or absence of 5 mM KCl, and the number of colonizing bacteria was counted. Shown are averages and SDs from 2 independent experiments with and n of ≥ 3 for each. (C) Seedlings were inoculated with either WT or $\Delta kinC$ *B. velezensis* FZB42 bacteria, for 48 h on 0.25× MS agar plates in the presence or absence of 5 mM KCl. Next, plates were inoculated with *R. solani* and incubated for an additional 7 days, and plant weight was measured. Untreated plants (neither bacteria nor fungi) were used as control. Shown are averages and SDs, $n \geq 20$. **, $P < 0.01$; ***, $P < 0.005$.

for bacterial survival in the natural environment and specifically, in the plant niche (9). Evolution of phage resistance has been associated with reduced host fitness on plants. An example is phage utilizing type IV pili (49), where the evolved mutant bacteria growly similar to the parental strain in planktonic culture but suffer from reduced biofilm formation and plant leaf colonization. Thus, it is important to explore phage-bacterium interactions in their natural context to gain insight into their coevolutionary dynamics.

Our genetic screen opens the way to discovering new phage resistance strategies that are not accessible during *in vitro* growth. An interesting future direction derives from the observation that among *in planta* phage-resistant bacteria, we found 4 of 100 with genetically inherited enhanced phage resistance. This suggests that 96% of the bacteria survived infection in a nongenetic manner. It would be interesting to determine how nongenetic mechanisms enable bacteria to survive phage infection. One possibility is by colonizing root niches that are less accessible to phage, a strategy that was recently demonstrated for phage infection of bacteria colonizing the gut ecosystem (50).

Potassium is an essential macronutrient for bacteria and plants. Unlike nitrogen and phosphate, it is not incorporated into cellular macromolecules but remains a soluble ion (51). Potassium is involved in the regulation of many processes, including osmotic

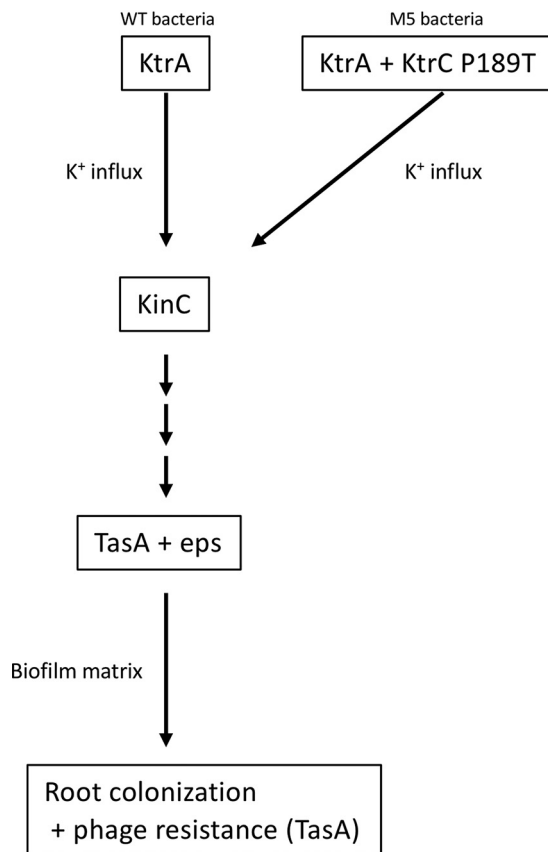


FIG 6 A model describing the effect potassium on root colonization and phage resistance.

adaptation, membrane potential, phloem transport, regulation of metabolic enzymes, and biotic and abiotic stress responses. Potassium, nitrogen, and phosphate, are the three main ions consumed by plants and are heavily utilized for fertilization in modern agriculture. (52). The effect of nitrogen and phosphorous on root microbial communities has been characterized (6, 53, 54). However, the role of potassium in bacterial colonization is less well explored. Our analysis suggests that addition of potassium is a simple method to enhance bacillus colonization. Many bacillus species exert positive effects on their plant host by enhancing plant growth and inhibiting pathogens. Our results suggest that adding potassium could enhance the ability of *B. velezensis* to protect seedlings from *R. solani* infection.

MATERIALS AND METHODS

Bacterial strains and growth conditions. WT *B. subtilis* NCBI 3610 and AR16 (55) (*B. subtilis* PY79) were kindly provided by Sigal Ben-Yehuda (Hebrew University); $\Delta tagE$ (BKK35730), $\Delta ktrA$ (BKK31090), $\Delta ktrC$ (BKK14510), and $\Delta kimA$ (BKK04320) strains (all in *B. subtilis* 168) were purchased from the Bacillus Genetic Stock Center (<http://www.bgsc.org/>). Genomic DNA was extracted from AR16 and mutant strains using a Wizard genomic DNA purification kit (Promega) and transformed into *B. subtilis* NCBI 3610. The media and growth conditions used for DNA transformation of *B. subtilis* NCBI 3610 are described at <http://2013.igem.org/Team:Groningen/protocols/Transformation>. The bacteria were cultivated routinely on Luria broth (LB) medium. When needed, the medium was solidified with 1.5% agar. For biofilm formation, bacteria grown overnight were inoculated into MSgg medium and incubated without shaking for 2 days at 30°C as described in reference 20. This medium was also solidified with 1.5% agar.

Phage strains and infection conditions. SPO1 (1P4) and SPP1 (1P7) phage were purchased from the Bacillus Genetic Stock Center. Phage lysate was routinely prepared by adding approximately 10^9 phage to mid-log cells grown in LB medium supplemented with 10 mM $MgSO_4$, until the culture was completely cleared. The lysate was then filtered through a 0.22- μ m Millipore filter. For lysis dynamics in LB medium (Fig. 2E and Fig. S1B), approximately 10^9 phage were added to mid-log-phase growing cells at multiplicity of infection (MOI) of 1, and the optical density at 600 nm (OD_{600}) was monitored at 30-min intervals. For SPO1 infection in pellicle biofilm (Fig. S3), bacteria grown overnight were inoculated into MSgg medium,

and phage was added at a MOI of 1. Bacteria were incubated without shaking for 2 days at 30°C, and the number of cultures with surviving cells was counted by eye. For SPO1 infection in solid biofilm (Fig. 4), bacteria grown overnight were inoculated into MSgg medium supplemented with 10⁵ PFU and solidified with 1.6% agar. A spot of 5 μ l from the bacterial culture was inoculated onto the plate and incubated for 2 days at 30°C. Plates were scanned and colony diameter was determined using ImageJ.

Monitoring bacterial growth and phage infection on plant roots. Plants were grown on 0.5 MS medium containing 1.1 g Murashige and Skoog basal salts (in 500 ml double-distilled water [ddH₂O]), 1% sucrose, 1% agar, and 5 ml (in 500 ml ddH₂O) morpholineethanesulfonic acid (MES; 50 g/liter, titrated to pH 5.8 with NaOH). Plants were stratified for 2 days in a 4°C dark room and grown vertically for 4 to 10 days under long-day light conditions. Bacteria from fresh colonies were grown in LB medium to an OD₆₀₀ of 1.0 and then diluted 1:100 in 1 \times phosphate-buffered saline (PBS) for CFU measurements and microscopy, yielding approximately 1 \times 10⁶. Phage were added to the 1 \times PBS at an MOI of 0.1 unless otherwise indicated. Six-day-old seedlings were transferred onto square petri dishes containing 0.5 MS but without sucrose. Two microliters of bacterial dilution was deposited immediately above the root tip and left to dry for 2 min. The square plates were kept in a vertical position during the incubation time at 22°C under long-day light conditions (16 h light/8 h darkness) in a plant growth chamber. For bacterial CFU counting and microscopy, plants were incubated with bacteria for 48 h. Then, the inoculated plant roots were cut and washed three times in sterile water. For CFU counting, the seedlings were transferred to a tube with 1 ml of 1 \times PBS and vortexed vigorously for 20 s; then, a serial dilution was plated on LB plates. For PFU measurement, roots were treated as described for CFU, but without the washing step.

Microscopy. Roots were observed using a Zeiss LSM 880 laser scanning confocal microscope with 20 \times lens objective. ConA₄₈₈ (Thermo Fisher C11252) staining was performed as described previously (26). Bacteria were observed using a Zeiss LSM 880 laser scanning confocal microscope with a 40 \times (water immersion) lens objective. Fluorescence intensity was measured using ImageJ.

DNA sequence analysis. DNA was extracted from an overnight culture of the mutant bacterial strain along with the WT strain using a DNeasy PowerSoil Pro kit (Qiagen), according to the manufacturer's instructions. DNA sequencing (DNA-seq) libraries were prepared using a Nextera DNA Flex library preparation kit (Illumina), according to the manufacturer's instructions. Illumina NextSeq 500 high-output 50-bp single reads were partially assembled into contigs using the SPAdes algorithm (56) with default parameters. The contigs were aligned to the genome of the WT bacteria from our lab stock.

Data analysis and statistics. All graphs and statistical tests were performed in Excel. *P* values throughout the paper were determined using Student's *t* test, except for Fig. S3, where a chi-square test was performed.

Data availability. All the data utilized to generate the graph can be found online at <https://www.doi.org/10.6084/m9.figshare.14925375>. The DNA-seq data set is available in the SRA repository under accession number PRJNA729435.

SUPPLEMENTAL MATERIAL

Supplemental material is available online only.

FIG S1, TIF file, 2.2 MB.

FIG S2, TIF file, 2.2 MB.

FIG S3, TIF file, 2.2 MB.

ACKNOWLEDGMENTS

We thank I. Taylor and E. Pierre-Jerome from the Benfey lab for critical reading of the manuscript. We also thank S. Ben-Yehuda (Hebrew university) for providing bacterial strains.

This work was supported by a grant from the NSF (PHY-1915445) to P.N.B., by the Howard Hughes Medical Institute to P.N.B., and by a BARD Postdoctoral Fellowship (FI-574-2018) to E.T.

REFERENCES

- Lundberg DS, Lebeis SL, Paredes SH, Yourstone S, Gehring J, Malfatti S, Tremblay J, Engelbrektson A, Kunin V, Del Rio TG, Edgar RC, Eickhorst T, Ley RE, Hugenholtz P, Tringe SG, Dangl JL. 2012. Defining the core *Arabidopsis thaliana* root microbiome. *Nature* 488:86–90. <https://doi.org/10.1038/nature11237>.
- Verbon EH, Liberman LM. 2016. Beneficial microbes affect endogenous mechanisms controlling root development. *Trends Plant Sci* 21:218–229. <https://doi.org/10.1016/j.tplants.2016.01.013>.
- Hacquard S, Garrido-Oter R, González A, Spaepen S, Ackermann G, Lebeis S, McHardy AC, Dangl JL, Knight R, Ley R, Schulze-Lefert P. 2015. Microbiota and host nutrition across plant and animal kingdoms. *Cell Host Microbe* 17:603–616. <https://doi.org/10.1016/j.chom.2015.04.009>.
- Lugtenberg B, Kamilova F. 2009. Plant-growth-promoting rhizobacteria. *Annu Rev Microbiol* 63:541–556. <https://doi.org/10.1146/annurev.micro.62.081307.162918>.
- Peiffer JA, Spor A, Koren O, Jin Z, Tringe SG, Dangl JL, Buckler ES, Ley RE. 2013. Diversity and heritability of the maize rhizosphere microbiome under field conditions. *Proc Natl Acad Sci U S A* 110:6548–6553. <https://doi.org/10.1073/pnas.1302837110>.
- Finkel OM, Salas-González I, Castrillo G, Spaepen S, Law TF, Teixeira PJPL, Jones CD, Dangl JL. 2019. The effects of soil phosphorus content on plant microbiota are driven by the plant phosphate starvation response. *PLoS Biol* 17:e3000534. <https://doi.org/10.1371/journal.pbio.3000534>.
- Wagner MR, Lundberg DS, Del Rio TG, Tringe SG, Dangl JL, Mitchell-Olds T. 2016. Host genotype and age shape the leaf and root microbiomes of a wild perennial plant. *Nat Commun* 7:12151. <https://doi.org/10.1038/ncomms12151>.
- Finkel OM, Salas-González I, Castrillo G, Conway JM, Law TF, Teixeira PJPL, Wilson ED, Fitzpatrick CR, Jones CD, Dangl JL. 2020. A single bacterial

- genus maintains root growth in a complex microbiome. *Nature* 587:103–108. <https://doi.org/10.1038/s41586-020-2778-7>.
9. Koskella B, Taylor TB. 2018. Multifaceted impacts of bacteriophages in the plant microbiome. *Annu Rev Phytopathol* 56:361–380. <https://doi.org/10.1146/annurev-phyto-080417-045858>.
 10. Koskella B, Brockhurst MA. 2014. Bacteria-phage coevolution as a driver of ecological and evolutionary processes in microbial communities. *FEMS Microbiol Rev* 38:916–931. <https://doi.org/10.1111/1574-6976.12072>.
 11. Salmond GP, Fineran PC. 2015. A century of the phage: past, present and future. *Nat Rev Microbiol* 13:777–786. <https://doi.org/10.1038/nrmicro3564>.
 12. Labrie SJ, Samson JE, Moineau S. 2010. Bacteriophage resistance mechanisms. *Nat Rev Microbiol* 8:317–327. <https://doi.org/10.1038/nrmicro2315>.
 13. Rodriguez-Valera F, Martin-Cuadrado A-B, Rodriguez-Brito B, Pasić L, Thingstad TF, Rohwer F, Mira A. 2009. Explaining microbial population genomics through phage predation. *Nat Rev Microbiol* 7:828–836. <https://doi.org/10.1038/nrmicro2235>.
 14. Buckling A, Rainey PB. 2002. The role of parasites in sympatric and allopatric host diversification. *Nature* 420:496–499. <https://doi.org/10.1038/nature01164>.
 15. Pal C, Macia MD, Oliver A, Schachar I, Buckling A. 2007. Coevolution with viruses drives the evolution of bacterial mutation rates. *Nature* 450:1079–1081. <https://doi.org/10.1038/nature06350>.
 16. Haaber J, Leisner JJ, Cohn MT, Catalan-Moreno A, Nielsen JB, Westh H, Penadés JR, Ingmer H. 2016. Bacterial viruses enable their host to acquire antibiotic resistance genes from neighbouring cells. *Nat Commun* 7:13333. <https://doi.org/10.1038/ncomms13333>.
 17. Paul JH, Sullivan MB. 2005. Marine phage genomics: what have we learned? *Curr Opin Biotechnol* 16:299–307. <https://doi.org/10.1016/j.copbio.2005.03.007>.
 18. Shkoporov AN, Hill C. 2019. Bacteriophages of the human gut: the “known unknown” of the microbiome. *Cell Host Microbe* 25:195–209. <https://doi.org/10.1016/j.chom.2019.01.017>.
 19. Pratama AA, van Elsas JD. 2018. The ‘neglected’ soil virome - potential role and impact. *Trends Microbiol* 26:649–662. <https://doi.org/10.1016/j.tim.2017.12.004>.
 20. Branda SS, Gonzalez-Pastor JE, Ben-Yehuda S, Losick R, Kolter R. 2001. Fruiting body formation by *Bacillus subtilis*. *Proc Natl Acad Sci U S A* 98:11621–11626. <https://doi.org/10.1073/pnas.191384198>.
 21. Stewart CR, Casjens SR, Cresawn SG, Houtz JM, Smith AL, Ford ME, Peebles CL, Hatfull GF, Hendrix RW, Huang WM, Pedulla ML. 2009. The genome of *Bacillus subtilis* bacteriophage SPO1. *J Mol Biol* 388:48–70. <https://doi.org/10.1016/j.jmb.2009.03.009>.
 22. Chen Y, Cao S, Chai Y, Clardy J, Kolter R, Guo J-h, Losick R. 2012. A *Bacillus subtilis* sensor kinase involved in triggering biofilm formation on the roots of tomato plants. *Mol Microbiol* 85:418–430. <https://doi.org/10.1111/j.1365-2958.2012.08109.x>.
 23. Beauregard PB, Chai Y, Vlamakis H, Losick R, Kolter R. 2013. *Bacillus subtilis* biofilm induction by plant polysaccharides. *Proc Natl Acad Sci U S A* 110: E1621–E1630. <https://doi.org/10.1073/pnas.1218984110>.
 24. Vlamakis H, Chai Y, Beauregard P, Losick R, Kolter R. 2013. Sticking together: building a biofilm the *Bacillus subtilis* way. *Nat Rev Microbiol* 11:157–168. <https://doi.org/10.1038/nrmicro2960>.
 25. Hoet PP, Coene MM, Cocito CG. 1992. Replication cycle of *Bacillus subtilis* hydroxymethyluracil-containing phages. *Annu Rev Microbiol* 46:95–116. <https://doi.org/10.1146/annurev.mi.46.100192.000523>.
 26. Habusha M, Tzipilevich E, Fiyaksel O, Ben-Yehuda S. 2019. A mutant bacteriophage evolved to infect resistant bacteria gained a broader host range. *Mol Microbiol* 111:1463–1475. <https://doi.org/10.1111/mmi.14231>.
 27. Brown S, Santa Maria JP, Jr, Walker S. 2013. Wall teichoic acids of Gram-positive bacteria. *Annu Rev Microbiol* 67:313–336. <https://doi.org/10.1146/annurev-micro-092412-155620>.
 28. Buckling A, Brockhurst M. 2012. Bacteria-virus coevolution. *Adv Exp Med Biol* 751:347–370. https://doi.org/10.1007/978-1-4614-3567-9_16.
 29. Allison SE, D’Elia MA, Arar S, Monteiro MA, Brown ED. 2011. Studies of the genetics, function, and kinetic mechanism of TagE, the wall teichoic acid glycosyltransferase in *Bacillus subtilis* 168. *J Biol Chem* 286:23708–23716. <https://doi.org/10.1074/jbc.M111.241265>.
 30. Banda J, Bellande K, von Wangenheim D, Goh T, Guyomarc’h S, Laplace L, Bennett MJ. 2019. Lateral root formation in *Arabidopsis*: a well-ordered L-Rexit. *Trends Plant Sci* 24:826–839. <https://doi.org/10.1016/j.tplants.2019.06.015>.
 31. Winstel V, Kühner P, Salomon F, Larsen J, Skov R, Hoffmann W, Peschel A, Weidenmaier C. 2015. Wall teichoic acid glycosylation governs *Staphylococcus aureus* nasal colonization. *mBio* 6:e00632. <https://doi.org/10.1128/mBio.00632-15>.
 32. Baptista C, Santos MA, Sao-Jose C. 2008. Phage SPP1 reversible adsorption to *Bacillus subtilis* cell wall teichoic acids accelerates virus recognition of membrane receptor YueB. *J Bacteriol* 190:4989–4996. <https://doi.org/10.1128/JB.00349-08>.
 33. Rocha R, Teixeira-Duarte CM, Jorge JMP, Morais-Cabral JH. 2019. Characterization of the molecular properties of KtrC, a second RCK domain that regulates a Ktr channel in *Bacillus subtilis*. *J Struct Biol* 205:34–43. <https://doi.org/10.1016/j.jsb.2019.02.002>.
 34. Corrigan RM, Campeotto I, Jegannathan T, Roelofs KG, Lee VT, Grundling A. 2013. Systematic identification of conserved bacterial c-di-AMP receptor proteins. *Proc Natl Acad Sci U S A* 110:9084–9089. <https://doi.org/10.1073/pnas.1300595110>.
 35. Gundlach J, Krüger L, Herzberg C, Turdiev A, Poehlein A, Tascón I, Weiss M, Hertel D, Daniel R, Hänelt I, Lee VT, Stülke J. 2019. Sustained sensing in potassium homeostasis: cyclic di-AMP controls potassium uptake by KimA at the levels of expression and activity. *J Biol Chem* 294:9605–9614. <https://doi.org/10.1074/jbc.RA119.008774>.
 36. Holtmann G, Bakker EP, Uozumi N, Bremer E. 2003. KtrAB and KtrCD: two K⁺ uptake systems in *Bacillus subtilis* and their role in adaptation to hypertonicity. *J Bacteriol* 185:1289–1298. <https://doi.org/10.1128/JB.185.4.1289-1298.2003>.
 37. Gundlach J, Herzberg C, Kaever V, Gunka K, Hoffmann T, Weiß M, Gibhardt J, Thürmer A, Hertel D, Daniel R, Bremer E, Commichau FM, Stülke J. 2017. Control of potassium homeostasis is an essential function of the second messenger cyclic di-AMP in *Bacillus subtilis*. *Sci Signal* 10:eal3011. <https://doi.org/10.1126/scisignal.aal3011>.
 38. Lopez D, Fischbach MA, Chu F, Losick R, Kolter R. 2009. Structurally diverse natural products that cause potassium leakage trigger multicellularity in *Bacillus subtilis*. *Proc Natl Acad Sci U S A* 106:280–285. <https://doi.org/10.1073/pnas.0810940106>.
 39. Grau RR, de Oña P, Kunert M, Leñini C, Gallegos-Monterrosa R, Mhatre E, Vileta D, Donato V, Hölscher T, Boland W, Kuipers OP, Kovács ÁT. 2015. A duo of potassium-responsive histidine kinases govern the multicellular destiny of *Bacillus subtilis*. *mBio* 6:e00581. <https://doi.org/10.1128/mBio.00581-15>.
 40. Bais HP, Fall R, Vivanco JM. 2004. Biocontrol of *Bacillus subtilis* against infection of *Arabidopsis* roots by *Pseudomonas syringae* is facilitated by biofilm formation and surfactin production. *Plant Physiol* 134:307–319. <https://doi.org/10.1104/pp.103.028712>.
 41. Fan B, Wang C, Song X, Ding X, Wu L, Wu H, Gao X, Borriss R. 2019. *Bacillus velezensis* FZB42 in 2018: the Gram-positive model strain for plant growth promotion and biocontrol. *Front Microbiol* 10:1279. <https://doi.org/10.3389/fmicb.2019.01279>.
 42. Kröber M, Wibberg D, Grosch R, Eikmeyer F, Verwaaijen B, Chowdhury SP, Hartmann A, Pühler A, Schlüter A. 2014. Effect of the strain *Bacillus amyloliquefaciens* FZB42 on the microbial community in the rhizosphere of lettuce under field conditions analyzed by whole metagenome sequencing. *Front Microbiol* 5:252. <https://doi.org/10.3389/fmicb.2014.00252>.
 43. Diaz-Munoz SL, Koskella B. 2014. Bacteria-phage interactions in natural environments. *Adv Appl Microbiol* 89:135–183. <https://doi.org/10.1016/B978-0-12-800259-9.00004-4>.
 44. Westra ER, van Houte S, Oyesiku-Blakemore S, Makin B, Broniewski JM, Best A, Bondy-Denomy J, Davidson A, Boots M, Buckling A. 2015. Parasite exposure drives selective evolution of constitutive versus inducible defense. *Curr Biol* 25:1043–1049. <https://doi.org/10.1016/j.cub.2015.01.065>.
 45. Moller AG, Lindsay JA, Read TD. 2019. Determinants of phage host range in staphylococcus species. *Appl Environ Microbiol* 85:e00209-19. <https://doi.org/10.1128/AEM.00209-19>.
 46. Vidakovic L, Singh PK, Hartmann R, Nadell CD, Drescher K. 2018. Dynamic biofilm architecture confers individual and collective mechanisms of viral protection. *Nat Microbiol* 3:26–31. <https://doi.org/10.1038/s41564-017-0050-1>.
 47. Hansen MF, Svenningsen SL, Roder HL, Middelboe M, Burmolle M. 2019. Big impact of the tiny: bacteriophage-bacteria interactions in biofilms. *Trends Microbiol* 27:739–752. <https://doi.org/10.1016/j.tim.2019.04.006>.
 48. Hall-Stoodley L, Costerton JW, Stoodley P. 2004. Bacterial biofilms: from the natural environment to infectious diseases. *Nat Rev Microbiol* 2:95–108. <https://doi.org/10.1038/nrmicro821>.
 49. Kim S, Rahman M, Seol SY, Yoon SS, Kim J. 2012. *Pseudomonas aeruginosa* bacteriophage PA10 requires type IV pili for infection and shows broad bactericidal and biofilm removal activities. *Appl Environ Microbiol* 78:6380–6385. <https://doi.org/10.1128/AEM.00648-12>.

50. Lourenço M, Chaffringeon L, Lamy-Besnier Q, Pédrón T, Campagne P, Eberl C, Bérard M, Stecher B, Debarbieux L, De Sordi L. 2020. The spatial heterogeneity of the gut limits predation and fosters coexistence of bacteria and bacteriophages. *Cell Host Microbe* 28:390.e5–401.e5. <https://doi.org/10.1016/j.chom.2020.06.002>.
51. Amtmann A, Armengaud P. 2009. Effects of N, P, K and S on metabolism: new knowledge gained from multi-level analysis. *Curr Opin Plant Biol* 12:275–283. <https://doi.org/10.1016/j.pbi.2009.04.014>.
52. Sustr M, Soukup A, Tylova E. 2019. Potassium in root growth and development. *Plants (Basel)* 8:435. <https://doi.org/10.3390/plants8100435>.
53. Leff JW, Jones SE, Prober SM, Barberán A, Borer ET, Firn JL, Harpole WS, Hobbie SE, Hofmockel KS, Knops JMH, McCulley RL, La Pierre K, Risch AC, Seabloom EW, Schütz M, Steenbock C, Stevens CJ, Fierer N. 2015. Consistent responses of soil microbial communities to elevated nutrient inputs in grasslands across the globe. *Proc Natl Acad Sci U S A* 112:10967–10972. <https://doi.org/10.1073/pnas.1508382112>.
54. Castrillo G, Teixeira PJL, Paredes SH, Law TF, de Lorenzo L, Feltcher ME, Finkel OM, Breakfield NW, Mieczkowski P, Jones CD, Paz-Ares J, Dangl JL. 2017. Root microbiota drive direct integration of phosphate stress and immunity. *Nature* 543:513–518. <https://doi.org/10.1038/nature21417>.
55. Rosenberg A, Sinai L, Smith Y, Ben-Yehuda S. 2012. Dynamic expression of the translational machinery during *Bacillus subtilis* life cycle at a single cell level. *PLoS One* 7:e41921. <https://doi.org/10.1371/journal.pone.0041921>.
56. Bankevich A, Nurk S, Antipov D, Gurevich AA, Dvorkin M, Kulikov AS, Lesin VM, Nikolenko SI, Pham S, Pribelski AD, Pyshkin AV, Sirotkin AV, Vyahhi N, Tesler G, Alekseyev MA, Pevzner PA. 2012. SPAdes: a new genome assembly algorithm and its applications to single-cell sequencing. *J Comput Biol* 19:455–477. <https://doi.org/10.1089/cmb.2012.0021>.